PHYSICAL REVIEW A VOLUME 32, NUMBER 1 JULY 1985

Laser-assisted charge-transfer reactions ($Li^{3+}+H$): Coupled dressed-quasimolecular-state approach

Tak-San Ho and Cecil Laughlin*
Department of Chemistry, University of Kansas, Lawrence, Kansas 66045-2112

Shih-I Chu
Department of Chemistry, University of Kansas,† Lawrence, Kansas 66045-2112
and Joint Institute for Laboratory Astrophysics, University of Colorado and National Bureau of Standards, Boulder, Colorado 80309

(Received 4 March 1985)

A semiclassical coupled dressed-quasimolecular-states (DQMS) approach is presented for *nonperturbative* treatment of *multichannel* charge-transfer reactions at *low* collision velocities and *high* laser intensities, incorporating the implementation of the generalized Van Vleck (GVV) nearly degenerate perturbation theory. The GVV technique allows block partitioning of the infinite-dimensional Floquet Hamiltonian into a finite-dimensional model DQMS space, and thereby reduces greatly the number of effective coupled channels. Further, the GVV-Floquet basis allows minimization of the (usually large in amplitude) field-induced nonadiabatic radial couplings without the need to explicitly construct the transformation between the adiabatic and diabatic DQMS basis. This yields a new set of coupled GVV-DQMS equations (neither adiabatic nor diabatic) which are particularly convenient for multichannel calculations. The method is applied to the study of the laser-assisted charge-transfer process: $Li^{3+}+H(1s)+\hbar\omega \rightarrow Li^{2+}(n=3)+H^+$, using 2-, 5-, and 15-GVV-DQMS basis. It is found that while the 5-state results agree well with the 15-state calculations even up to very high intensities for the $(LiH)^{3+}$ system, the 2-state basis is inadequate at high-intensity and lower-wavelength regimes. Detailed results and nonlinear dynamical features are presented for the process at small impact velocity 10^7 cm/s and strong laser fields with intensity ranging from 1 to 100 TW/cm^2 and wavelengths from 1500 to 3000 Å.

I. INTRODUCTION

Knowledge of the charge-transfer cross sections in ion-atom collisions plays an important role in the interpretation and understanding of many physical phenomena such as determining the radiation losses and neutral beam heating efficiencies in tokamak plasmas[1] and predicting the feasibility of producing an x-ray laser.[2]

It is known that the nonresonant ion-atom charge-transfer cross section, which is normally small at low velocities, can be enhanced a great deal by the presence of a strong laser field.[3] The observation of a laser-induced charge-exchange collision involving Ca^+ and Sr has also been reported.[4] More recently, Seely and Elton[5] have suggested that photon-induced charge-transfer reactions are also useful for the measurement of particle densities, with time and space resolution provided by the pumping laser beam, in a tokamak plasma.

Theoretical studies[6–12] have shown that at weak laser fields and at small impact velocities, the laser assisted processes $A^+ + B + \hbar\omega \rightarrow A + B^+$ can be well described by perturbative schemes of one kind or another within the rotating-wave approximation (RWA) and the impact-parameter formalism, and that the charge-transfer cross sections behave linearly as a function of the intensity of the laser field and as a function of the reciprocal of the impact velocity. These approaches, however, are generally difficult to extend to high laser intensity and very low collision velocity regions where the laser-induced charge-transfer rates tend to be the largest. In a previous paper,[13] hereafter called paper I, the authors have developed a nonperturbative *coupled dressed-quasimolecular-states* (DQMS) approach for the treatment of charge-transfer processes at low collision velocities and strong laser intensities. The theory parallels an earlier treatment developed by one of us[14] in the study of multiphoton enhancement of vibrational excitations induced by molecular collisions. The essence of the coupled DQMS approach is as follows: As the laser frequency of interest is in the range of quasimolecular electronic energy separations, the laser field oscillates more rapidly than the nuclear motion. It is then legitimate to first construct the solutions of the $(A\text{-}B)^+ +$ field system, namely, the dressed quasimolecular electronic states (also called the quasienergy or electronic-field states) with the internuclear separation R fixed. The laser-assisted collision processes can then be treated as the electronic transitions among the DQMS driven by the nuclear motion only. The DQMS can be determined by invoking either the full quantized treatment[15] or the semiclassical Floquet theory,[16,17] both treatments being equivalent in strong fields.[16(a)] In our approach, we have adopted the Floquet approach, which has been extensively used recently in studies of multiphoton excitation and dissociation of molecules.[17]

The DQMS obtained via the Floquet theory are *adiabatic,* and their associated quasienergies (depending

parametrically on R) exhibit regions of avoided crossings, where the electronic transition probabilities are large due to the strong radial couplings induced by nuclear movement. By further transforming the *adiabatic* DQMS into an appropriate *diabatic* DQMS representation, defined via the vanishing of the radial couplings (through the unitary transformation of Smith[18(a)] and Heil and Dalgarno[18(b)]), we obtained a new set of coupled (diabatic DQMS) equations, which offer some computational advantages. The above-mentioned procedure has been extended to the study of the laser-assisted charge-exchange process $He^{2+}+H(1s)+\hbar\omega\rightarrow He^{+}(n=2)+H^{+}$, in a two-state approximation but beyond the RWA, for the velocity range from 1.5×10^{5} to 2×10^{7} cm/s, and for the laser intensity in the range of 0.4 to 4.0 TW/cm^2.

In this paper we further exploit the DQMS approach with particular emphasis on more complex systems where the number of coupled DQMS is large particularly at high laser intensities. We shall focus on developing new techniques which are capable of reducing the number of coupled channels and at the same time providing numerically stable algorithms for multichannel calculations. One notices that the infinite-dimensional Floquet matrix (or the fully quantized Hamiltonian) can be partitioned in such a way that nearly degenerate Floquet (dressed) states form a closely coupled subspace (called the model space) which can be decoupled from the rest of the Floquet states (called the external space) to any desired order of perturbation theory. One of the major goals of this paper is to extend the generalized Van Vleck (GVV) nearly degenerate perturbation theory[19,20] to block-partition the infinite-dimensional Floquet Hamiltonian to a finite-dimensional model-space Hamiltonian, thereby reducing greatly the number of coupled channels in the laser-assisted charge-exchange studies. Although the GVV-Floquet basis, which defines the partitioned model space spanned by the nearly degenerate states of interest, is not the same diabatic basis defined exactly in the sense of Smith[18(a)] and Heil and Dalgarno,[18(b)] we shall show that the GVV basis minimizes the part of the radial coupling matrix which is mainly provoked by the resonant laser field, and therefore reduces the coupled adiabatic DQMS equations to coupled diabatic DQMS equations when the collision-induced couplings are neglected.

Of particular interest is the charge-transfer process $Li^{3+}+H(1s)+n\hbar\omega\rightarrow Li^{2+}(n=3)+H^{+}$ which (1) is of relevance in controlled thermonuclear fusion research, and (2) involves a large number of the dressed-quasimolecular states, thus providing a good test case for the present approach. The same process has been recently studied by Errea *et al.*[11(b)] using a first-order perturbative approach and two-state model within the RWA. As will be demonstrated later, while the two-state model is adequate for certain low laser intensity ($I<1$ TW/cm^2) and some smaller frequency ranges, one needs in general to consider many more quasimolecular states to obtain converged results, thus demanding more elaborate treatment such as the coupled DQMS approach presented here.

In Sec. II, we first briefly review the coupled DQMS approach developed in paper I,[13] and then formulate the coupled GVV-DQMS equations, based on the generalized Van Vleck nearly degenerate perturbation theory. The comparisons between the GVV approach and the previous coupled adiabatic and diabatic DQMS approaches are elaborated based on a *nonperturbative* two-state model in Sec. III. The laser-assisted process $Li^{3+}+H(1s)+n\hbar\omega\rightarrow Li^{2+}(n=3)+H^{+}$ is studied in detail based on three nonperturbative models: the 2-state (2S), the 5-state (5S), and the 15-state (15S) in Sec. IV. This is followed by a conclusion in Sec. V. Atomic units will be used throughout the paper unless otherwise specified.

II. THEORY

A. The dressed-quasimolecular-state approach

Within the semiclassical trajectory formulation and the electric dipole approximation, the slow ion-atom collisions in the presence of an intense linearly polarized laser field can be described by the time-dependent Schrödinger equation

$$i\frac{\partial}{\partial t}\Psi(\mathbf{r},t\mid\mathbf{R}(t))=\hat{H}(\mathbf{r},t\mid\mathbf{R}(t))\Psi(\mathbf{r},t\mid\mathbf{R}(t)) , \tag{1}$$

where $\Psi(\mathbf{r},t\mid\mathbf{R}(t))$ is the state wave function of the colliding system at some instant of the time t, and $\hat{H}(\mathbf{r},t\mid\mathbf{R}(t))$, the total Hamiltonian, is composed of a field-free electron Hamiltonian $\hat{h}_{\rm el}(\mathbf{r}\mid\mathbf{R}(t))$ and an interaction $\hat{V}(\mathbf{r},t)=-\mathbf{r}\cdot\mathbf{E}_0\cos(\omega t)$ between the active electron, positioned at $\mathbf{r}$, and the applied laser field of frequency ω and amplitude $\mathbf{E}_0(\theta,\phi)$ whose orientation is given by the polar and azimuthal angles θ and ϕ, respectively. The $\hat{\mathbf{z}}$ direction is chosen parallel to the initial impact velocity $\mathbf{v}_0$ of the two nuclei. The nuclear trajectory $\mathbf{R}(t)$ is determined by some average potential of the two colliding entities, and will be taken as rectilinear, as in the impact-parameter method, in the rest of the test for simplicity. Therefore, for each specified impact parameter $\mathbf{b}\perp\mathbf{v}_0$, we have $\mathbf{R}(t)=\mathbf{b}+\mathbf{v}_0t$. Assuming that the frequency of the laser field is of the same order of magnitude as that characterizing the electronic motion, i.e., much greater than that characterizing the nuclear motion, the electronic states can be first thought of as being dressed by the applied laser field before adjusting to the changing molecular field caused by the nuclear motion. The DQMS wave function $\phi^{a}_{\beta n}(\mathbf{r},t\mid\mathbf{R}(t))$ obeys the eigenvalue equation obtained by the Floquet theorem[13]

$$\left[\hat{H}-i\left[\frac{\partial}{\partial t}\right]_{\mathbf{R}}\right]\phi^{a}_{\beta n}(\mathbf{r},t\mid\mathbf{R}(t)) =\epsilon^{a}_{\beta n}(R(t))\phi^{a}_{\beta n}(\mathbf{r},t\mid\mathbf{R}(t)) \tag{2}$$

defined in an extended Hilbert space $R\oplus T$ with the spatial part R spanned by the eigenfunctions $\psi_\beta(\mathbf{r}\mid\mathbf{R}(t))$ of the field-free electronic Schrödinger equation

$$\hat{h}_{\rm el}(\mathbf{r}\mid\mathbf{R})\psi_\beta=E_\beta(R)\psi_\beta,\quad \beta=1,2,\ldots,N \tag{3}$$

and the temporal part T by the complete orthonormal set of functions $e^{in\omega t}$, $n=0,\pm1,\pm2,\ldots\pm\infty$, which obey the relation

$$\frac{\omega}{2\pi}\int_0^{2\pi/\omega} e^{i(m-n)\omega t}dt=\delta_{mn}\ . \tag{4}$$

The time derivative $(\partial/\partial t)_{\mathbf{R}}$ in Eq. (2) is taken at some fixed internuclear distance $\mathbf{R}$. The DQMS potential energies $\epsilon^a_{\beta n}(R(t))$ thus adjust continuously to the change of the internuclear separation R. By expanding the total wave function $\Psi(\mathbf{r},t\mid\mathbf{R}(t))$ of Eq. (1) in terms of the DQMS wave functions $\phi^a_{\beta n}(\mathbf{r},t\mid\mathbf{R}(t))$, i.e.,

$$\Psi(\mathbf{r},t\mid\mathbf{R}(t))=\sum_{\beta,n}\chi^a_{\beta n}(\mathbf{R}(t))\phi^a_{\beta n}(\mathbf{r},t\mid\mathbf{R}(t)) \tag{5}$$

and inserting it into Eq. (1) we obtain a set of coupled *adiabatic* DQMS equations for $\chi^a_{\beta n}(\mathbf{R}(t))$, namely,

$$i\frac{\partial}{\partial t}\chi^a_{\beta n}(R(t))=\epsilon^a_{\beta n}(R(t))\chi^a_{\beta n}(\mathbf{R}(t)) -i\dot{\mathbf{R}}\cdot\sum_{\alpha,m}\hat{\mathbf{A}}^{\,a}_{\beta n,\alpha m}(\mathbf{R}(t))\chi^a_{\alpha m}(\mathbf{R}(t))\ , \tag{6}$$

where the nonadiabatic coupling matrix element $\hat{\mathbf{A}}^{\,a}_{\beta n,\alpha m}(\mathbf{R}(t))$ between two arbitrary DQMS wave functions $\phi^a_{\beta n}(\mathbf{r},t\mid\mathbf{R}(t))$ and $\phi^a_{\alpha m}(\mathbf{r},t\mid\mathbf{R}(t))$ can be written as

$$\hat{\mathbf{A}}^{\,a}_{\beta n,\alpha m}(\mathbf{R}(t))\equiv\langle\langle\phi^a_{\beta n}\mid\nabla_{\mathbf{R}}\mid\phi^a_{\alpha m}\rangle\rangle_R =\frac{\omega}{2\pi}\int_0^{2\pi/\omega}dt\int d\mathbf{r}\,\phi^a_{\beta n}\nabla_{\mathbf{R}}\phi^a_{\alpha m}\ . \tag{7}$$

Equation (2) can be solved by expanding the DQMS wave function $\phi^a_{\beta n}(\mathbf{r},t\mid\mathbf{R}(t))$, which is a periodic function of t with period $2\pi/\omega$ at each fixed internuclear separation R, i.e., $\phi^a_{\beta n}(\mathbf{r},t+2\pi/\omega\mid\mathbf{R})=\phi^a_{\beta n}(\mathbf{r},t\mid\mathbf{R})$, in terms of the field-free quasimolecular-state wave functions $\{\psi_\alpha\}$ and the Fourier basis $\{e^{im\omega t}\}$,

$$\phi^a_{\beta n}(\mathbf{r},t\mid\mathbf{R})=\sum_{\alpha,m}\langle\alpha m\mid\epsilon^a_{\beta n}\rangle e^{im\omega t}\psi_\alpha(\mathbf{r},\mathbf{R})\ . \tag{8}$$

Here the expansion coefficient $\langle\alpha m\mid\epsilon^a_{\beta m}\rangle$ satisfies an infinite-dimensional eigenvalue equation

$$\sum_\gamma\sum_k\langle\alpha m\mid\hat{H}_F\mid\gamma k\rangle\langle\gamma k\mid\epsilon^a_{\beta n}\rangle=\epsilon^a_{\beta n}(R)\langle\alpha m\mid\epsilon^a_{\beta n}\rangle \tag{9}$$

with the Floquet Hamiltonian $\hat{H}_F$ at each fixed R defined as

$$\langle\alpha m\mid\hat{H}_F\mid\gamma k\rangle(R)=E_\alpha(R)\delta_{\alpha\gamma}\delta_{mk}+m\omega\delta_{\alpha\gamma}\delta_{mk} -\frac{\mathbf{E}_0}{2}\cdot\langle\psi_\alpha\mid\mathbf{r}\mid\psi_\gamma\rangle(\delta_{m,k+1}+\delta_{m,k-1}). \tag{10}$$

In terms of coefficients $\{\langle\alpha m\mid\epsilon^a_{\beta n}\rangle(R)\}$ the nonadiabatic coupling matrix elements $\hat{\mathbf{A}}^{\,a}_{\beta n,\alpha m}(\mathbf{R})$ can be written as

$$\hat{\mathbf{A}}^{\,a}_{\beta n,\alpha m}(\mathbf{R})=\hat{\mathbf{B}}^{\,a}_{\beta n,\alpha m}(\mathbf{R})+\hat{\mathbf{D}}^{\,a}_{\beta n,\alpha m}(\mathbf{R})\ , \tag{11}$$

where the field-dominated coupling

$$\hat{\mathbf{B}}^{\,a}_{\beta n,\alpha m}(\mathbf{R})=\frac{\mathbf{R}}{R}\sum_\gamma\sum_k\langle\epsilon^a_{\beta n}\mid\gamma k\rangle\frac{d}{dR}\langle\gamma k\mid\epsilon^a_{\alpha m}\rangle \tag{12}$$

and the collision-dominated coupling

$$\hat{\mathbf{D}}^{\,a}_{\beta n,\alpha m}(\mathbf{R}) =\sum_{\gamma_2}\sum_{\gamma_1}\sum_k\langle\epsilon^a_{\beta n}\mid\gamma_2 k\rangle\langle\gamma_1 k\mid\epsilon^a_{\alpha m}\rangle\langle\psi_{\gamma_2}\mid\nabla_{\mathbf{R}}\mid\psi_{\gamma_1}\rangle\ . \tag{13}$$

Here we note that the coefficient $\langle\gamma k\mid\epsilon^a_{\beta n}\rangle$ depends only on the internuclear separation R and can be obtained easily by diagonalizing a truncated, yet converged, Floquet Hamiltonian $\hat{H}_F(R)$ defined by Eq. (10), while the field-free nonadiabatic coupling $\langle\psi_{\gamma_2}\mid\nabla_{\mathbf{R}}\mid\psi_{\gamma_1}\rangle$ in general depends on both the amplitude and the direction of the vector $\mathbf{R}$. The field-dominated coupling $\hat{\mathbf{B}}^{\,a}_{\beta n,\alpha m}(\mathbf{R})$ becomes important when the two field-free electronic states, denoted by $E_\beta(R)$ and $E_\alpha(R)$, are strongly mixed by the applied laser field, i.e., the corresponding Rabi frequency $|-\frac{1}{2}\langle\psi_\beta\mid\mathbf{r}\mid\psi_\alpha\rangle\cdot\mathbf{E}_0|$ is larger than or comparable with the detuning $\Delta_{\beta\alpha}(R)=|E_\beta(R)-E_\alpha(R)|-\omega$. The collision-dominated coupling $\hat{\mathbf{D}}^{\,a}_{\beta n,\alpha m}(\mathbf{R})$ becomes significant only when the corresponding field-free electronic potential energies $E_\beta(R)$ and $E_\alpha(R)$ possess pseudocrossings, at some internuclear separation R. In the DQMS representation, cf. Eq. (6), states which are strongly coupled are thus indicated by regions of avoided crossings, a manifestation of the size of either $\hat{\mathbf{B}}^{\,a}_{\beta n,\alpha m}(\mathbf{R})$, or $\hat{\mathbf{D}}^{\,a}_{\beta n,\alpha m}(\mathbf{R})$, or both, in the correlation diagram of the DQMS potential energies $\epsilon^a_{\beta n}(R)$. Therefore, in the coupled adiabatic DQMS equation (6), the collision-induced and the field-induced transition mechanisms are treated on an equal footing. We note also that as long as the collision-dominated coupling $\hat{\mathbf{D}}^{\,a}$ is small when compared with the field-dominated coupling $\hat{\mathbf{B}}^{\,a}$, the inclusion of electronic translational factors (not treated here) is not essential and has no significant effect on the field-assisted charge-exchange rates.

A particularly interesting case is that where the collision-induced coupling $\hat{\mathbf{D}}^{\,a}_{\beta n,\alpha m}(\mathbf{R})$ can be completely ignored and the field-induced coupling, provoked either by single-, or multiple-photon resonant transitions at some finite internuclear distances R_x, is solely important, e.g., the laser-assisted charge-transfer process at very slow collision velocities

$$\mathrm{Li}^{3+}+\mathrm{H}(1s)+n\hbar\omega\rightarrow\mathrm{Li}^{2+}(n=3)+\mathrm{H}^+\ . \tag{14}$$

In the process (14), the field-free electronic correlation diagram shows no pseudocrossing between potential energies of the entrance and exit channels, see Fig. 1(a),[21] and the collision-induced coupling is thus negligible. When the laser, whose frequency matches the electronic energies of the entrance channel, i.e., $3d\sigma$ state in the process (14), and the reactive channels, i.e., $4f\sigma$, $3d\pi$, $3p\sigma$, and $3p\pi$ states, at some internuclear distance R_x where the transition dipole moments are nonvanishing, see Figs. 1(a) and 1(b), is turned on adiabatically, large transitions between these channels can take place via the absorption or emission of photons during the collision. More vividly, the transitions between various DQMS states are dictated by the DQMS correlation diagram,[21] shown in Fig. 2. In Fig. 2 we see that the usual simple picture of the close-coupling approach in field-free slow ion (atom)-atom col-

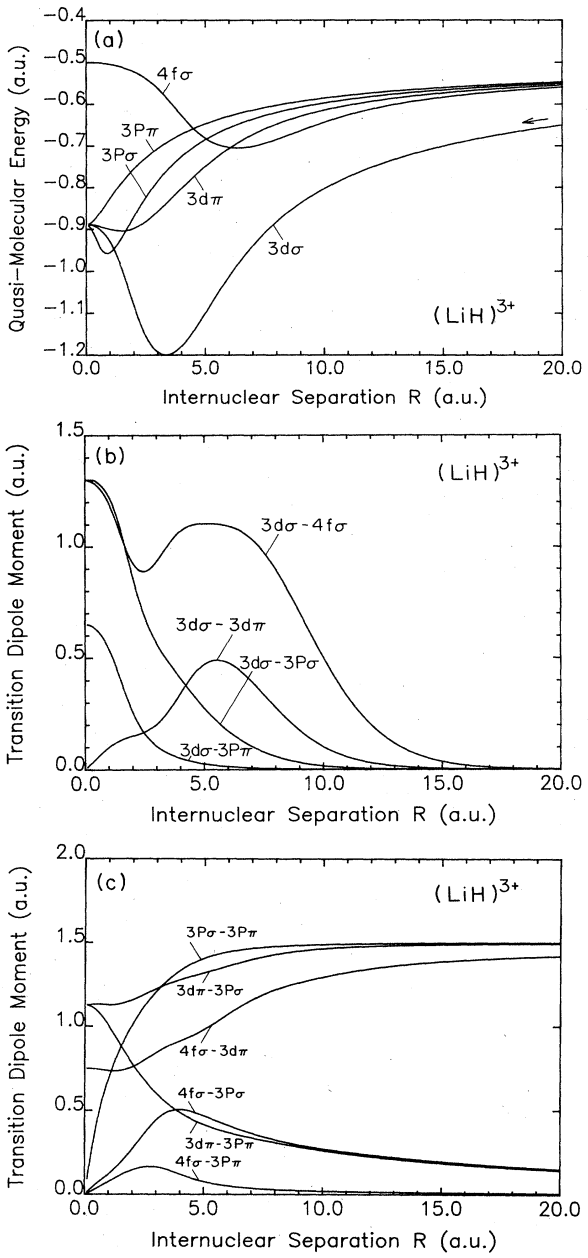

FIG. 1. (a) The field-free quasimolecular electronic energies of the $3d\sigma$, $3d\pi$, $3p\sigma$, $3p\pi$, and $4f\sigma$ states of the $(LiH)^{3+}$ system. (b) and (c) are electronic transition dipole moments.

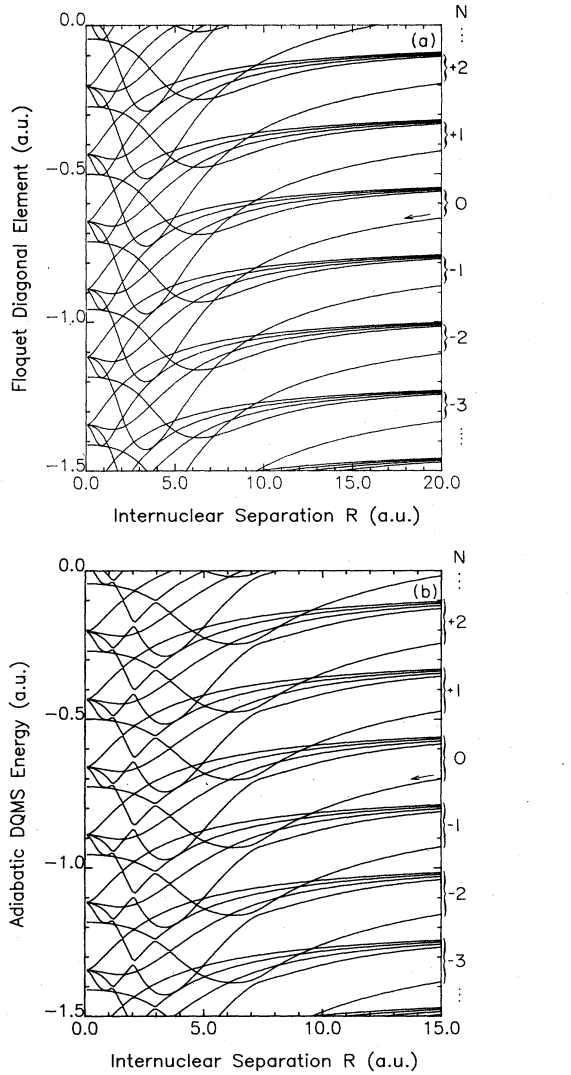

FIG. 2. (a) The Floquet diagonal elements $E_\alpha(R)+m\omega$ and (b) the adiabatic DQMS energies $\epsilon^a_{\alpha m}(R)$ of the $(LiH)^{3+}$ + field system at impact parameter $\rho=0.1$ a.u., field intensity $I=10$ TW/cm^2 (the field $\mathbf{E}_0||\hat{\mathbf{z}}$), and field wavelength $\lambda=2000$ Å. Indices appearing on right-hand side denote the Floquet photon blocks to which the levels bracketed belong.

lisions can be greatly complicated by the appearance of the laser field. Further, the endothermic and inactive (field-free) process, namely,

$$Li^{3+}+H(1s)\rightarrow Li^{2+}(n=3)+H^+$$

can become very dynamic in the presence of a resonant laser field.

To illustrate the salient features of the field-induced coupling $\hat{\mathbf{B}}^a_{\beta n,\alpha m}(\mathbf{R})$, or $\hat{\mathbf{A}}^a_{\beta n,\alpha m}(\mathbf{R})$ in general, we assume that only the transition dipole moments depicted in Fig. 1(b) are important and present the correlation diagram of intimately coupled DQMS potential energies in Fig. 3(a) and the corresponding field-induced couplings in Fig. 3(b). In regions of avoided crossings, see Fig. 3(a), the associated nonadiabatic couplings $\hat{\mathbf{A}}^a_{\beta n,\alpha m}(\mathbf{R})$ are either extended and small, or narrow and high-rising, depending on the degree to which the coupled states are mixed. An alternative procedure which avoids the numerical complexity of the nonadiabatic couplings is to transform the adiabatic DQMS basis $\{\phi^a_{\beta n}\}$ into a diabatic DQMS basis $\{\phi^d_{\beta n}\}$ such that the corresponding coupling matrix element of the operator $\nabla_{\mathbf{R}}$ vanish, and the result is a set of coupled *diabatic* DQMS equations,[13] namely,

$$i\frac{\partial}{\partial t}\chi^d_{\beta n}(\mathbf{R}(t))=\sum_\alpha\sum_m V_{\beta n,\alpha m}(\mathbf{R}(t))\chi^d_{\alpha m}(\mathbf{R}(t)) . \quad (15)$$

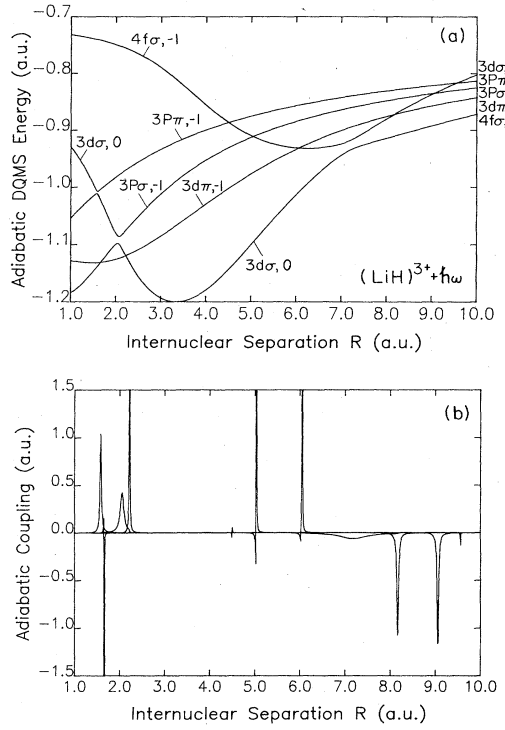

FIG. 3. (a) The adiabatic DQMS energies $\epsilon^a_{\alpha m}(R)$ of the $(LiH)^{3+}$ + field system under the five-state model and (b) the corresponding adiabatic couplings $|\dot{\mathbf{R}}\cdot\hat{\mathbf{B}}^{(a)}_{\beta n,\alpha m}|$ of Eq. (12) at impact parameter $\rho=1.0$ a.u., impact velocity $|\mathbf{v}_0|=1.0\times10^7$ cm/s, field intensity $I=10$ TW/cm^2, and field wavelength $\lambda=2000$ Å.

Here the $\chi^d_{\beta n}(\mathbf{R}(t))$ are the coefficients in the expansion of the total wave function $\Psi(\mathbf{r},t\,|\,\mathbf{R}(t))$ of Eq. (1) in terms of the complete set of diabatic DQMS functions $\{\phi^d_{\beta n}(\mathbf{r},t\,|\,\mathbf{R}(t))\}$, namely,

$$\Psi(\mathbf{r},t\,|\,\mathbf{R}(t))=\sum_{\beta,n}\chi^d_{\beta n}(\mathbf{R}(t))\phi^d_{\beta n}(\mathbf{r},t\,|\,\mathbf{R}(t)) \tag{16}$$

and the diabatic potential $\hat{V}_{\beta n,\alpha m}(\mathbf{R})$ is given by

$$\hat{V}_{\beta n,\alpha m}(\mathbf{R})=\sum_{\gamma}\sum_{k}(\hat{C}^{-1})_{\beta n,\gamma k}\epsilon^a_{\gamma k}(R)\hat{C}_{\gamma k,\alpha m}\ . \tag{17}$$

The matrix $\hat{C}$ in Eq. (17) is defined by the relation[18(b)]

$$\sum_{\gamma}\sum_{k}\hat{\mathbf{A}}^{\,a}_{\alpha m,\gamma k}(\mathbf{R})\hat{C}_{\gamma k,\beta n}(R)+\frac{d}{dR}\hat{C}_{\alpha m,\beta n}(R)=0 \tag{18}$$

and provides the transformation between the diabatic and adiabatic DQMS wave functions

$$\phi^d_{\beta n}(\mathbf{r},t\,|\,\mathbf{R})=\sum_{\alpha}\sum_{m}\phi^a_{\alpha m}(\mathbf{r},t\,|\,\mathbf{R})\hat{C}_{\alpha m,\beta n}(R)\ . \tag{19}$$

As shown in paper I,[13] the diabatic potentials $\hat{V}_{\beta n,\alpha m}(R)$ thus constructed are in general much smoother and smaller in magnitude when compared with the nonadiabatic couplings $\hat{\mathbf{A}}^{\,a}_{\beta n,\alpha m}(R)$. Hence numerical solutions of the coupled diabatic DQMS equations, Eqs. (15), are usually easier to perform than the corresponding coupled adiabatic equations, Eqs. (6). However, as can be seen from Fig. 3, the transformation from the adiabatic to a diabatic basis and therefore the construction of the diabatic potentials for the *multichannel* case is nontrivial and may be in fact sometimes difficult to perform. In the Sec. III B we introduce an alternative way to minimize the nonadiabatic couplings $\hat{\mathbf{A}}^{\,a}_{\beta n,\alpha m}$ without the need to explicitly construct the transformation between the adiabatic and diabatic basis.

B. The generalized Van Vleck nearly degenerate perturbation approach

In a recent paper,[22] we have extended the GVV nearly degenerate perturbation theory[19,20] to study the multiphonon excitation dynamics of finite-level systems in strong laser fields. For a laser-assisted reaction, e.g., Eq. (14), in the slow ion (atom)-atom collisions, the enhancement of the reaction rate is mainly caused by resonant single (or multiple)-photon transitions in regions where the laser frequency (or its harmonics) is close to the energy defect, say $|E_\beta(R_x)-E_\alpha(R_x)|$, of two field-free quasimolecular states possessing significant transition dipole moments. From the DQMS correlation diagram, e.g., Fig. 2, we see that once the entrance channel is selected, only some finite number (which may be large) of nearly degenerate dressed-quasimolecular states will be significant at various stages of the collision. Therefore in solving the time-independent [but implicitly depending on time via $\mathbf{R}(t)$] eigenvalue equation (9), which is equivalent to the Schrödinger equation (2), with $\mathbf{R}$ fixed, we can partition the total Floquet Hamiltonian $\hat{H}_F(R)$ of Eq. (10) into two parts: one, M_0, consists of unperturbed DQMS states (including the entrance channel) which are nearly degenerate in the course of the collision, and two, W_0, consists of the rest of the states. By invoking the GVV approach we construct a model space M spanned by some perturbed model-space wave functions with each of them, to the zeroth order, reducing to one of the states in M_0. The total Floquet Hamiltonian $\hat{H}_F(R)$ can then be block-diagonalized by the model-space functions, or equivalently the model-space wave functions can be made orthogonal to the external-space wave functions in W, to any desired order of perturbation theory. Therefore the laser-assisted collisions of the kind discussed in this paper can be confined to a finite-dimensional subspace, the model space M defined above in the GVV theory.

For convenience we shall abbreviate unperturbed DQMS states which span M_0 by $|A\rangle$, $|B\rangle$, $|C\rangle,\ldots,$ and the rest which span W_0 by $|I\rangle$, $|J\rangle$, $|K\rangle,\ldots,$ instead of using double indices like $|\alpha m\rangle$, $|\beta n\rangle$, $|\gamma k\rangle,\ldots$ appearing in Eqs. (8), (9), and (10). According to the GVV theory we form a model space M from perturbed model-space wave functions

$$|\lambda_{A'}(R)\rangle=|\lambda^{(0)}_{A'}(R)\rangle+|\lambda^{(1)}_{A'}(R)\rangle+|\lambda^{(2)}_{A'}(R)\rangle+\cdots,\quad A'=A,B,C,\ldots \tag{20}$$

where $|\lambda^{(0)}_{A'}(R)\rangle\equiv|A'\rangle$. Correspondingly, the perturbed external-space wave functions can be written as

$$|\xi_I(R)\rangle = |\xi_I^{(0)}(R)\rangle + |\xi_I^{(1)}(R)\rangle + |\xi_I^{(2)}(R)\rangle + \cdots , \quad I = I,J,K,\ldots \tag{21}$$

where $|\xi_I^{(0)}\rangle \equiv |I\rangle$. The eigenfunctions $\{|\epsilon_{\alpha m}^a\rangle\}$ which diagonalize the total Floquet Hamiltonian $\hat{H}_F(R)$ within the manifold M can then be related to the model-space wave functions $\{|\lambda_A\rangle\}$ by a unitary transformation $\hat{U}$, namely,

$$|\lambda_A\rangle = \sum_\alpha \sum_m \hat{U}_{\alpha m,A}(R)\,|\epsilon_{\alpha m}^a\rangle \tag{22}$$

with $\hat{U}^\dagger = \hat{U}^{-1}$. The transformation defined in Eq. (22) amounts to

$$\phi_A^{(\mathrm{GVV})}(\mathbf{r},t\,|\,\mathbf{R}) = \sum_\alpha \sum_m \hat{U}_{\alpha m,A}(R)\phi_{\alpha m}^a(\mathbf{r},t\,|\,\mathbf{R}) \tag{23}$$

which gives a new basis $\{\phi_A^{(\mathrm{GVV})}(\mathbf{r},t\,|\,\mathbf{R})\}$. By approximating the total wave function $\Psi(\mathbf{r},t\,|\,\mathbf{R}(t))$ as a linear superposition of the transformed wave functions $\{\phi_A^{(\mathrm{GVV})}(\mathbf{r},t\,|\,\mathbf{R})\}$,

$$\Psi(\mathbf{r},t\,|\,\mathbf{R}(t)) \cong \sum_A \chi_A^{(\mathrm{GVV})}(\mathbf{R})\phi_A^{(\mathrm{GVV})}(\mathbf{r},t\,|\,\mathbf{R}) , \tag{24}$$

we obtain a finite set of coupled equations,

$$i\frac{\partial}{\partial t}\chi_A^{(\mathrm{GVV})}(\mathbf{R}(t)) = \sum_B \hat{H}_{A,B}^{(\mathrm{GVV})}\chi_B^{(\mathrm{GVV})} - i\dot{\mathbf{R}}\cdot\sum_B \hat{\mathbf{A}}_{A,B}^{(\mathrm{GVV})}\chi_B^{(\mathrm{GVV})} . \tag{25}$$

The GVV Hamiltonian $\hat{H}^{(\mathrm{GVV})}$ in Eq. (25) can be evaluated directly once the model-space wave functions $\{|\lambda_A\rangle\}$ are obtained, and can be related to the exact DQMS energies $\{\epsilon_{\alpha m}^a(R)\}$ by the relation

$$\hat{H}_{A,B}^{(\mathrm{GVV})}(\mathbf{R}) = \sum_\alpha \sum_m (\hat{U}^\dagger)_{A,\alpha m}\epsilon_{\alpha m}^a(R)\hat{U}_{\alpha m,B} . \tag{26}$$

The matrix $\hat{\mathbf{A}}^{(\mathrm{GVV})}(\mathbf{R})$, which is the counterpart of the $\hat{A}^a(\mathbf{R})$ in Eq. (6), can be written explicitly as

$$\hat{\mathbf{A}}_{A,B}^{(\mathrm{GVV})}(\mathbf{R}) = \frac{\mathbf{R}}{R}\sum_\gamma \sum_k \langle\lambda_A\,|\,\gamma k\rangle\frac{d}{dR}\langle\gamma k\,|\,\lambda_B\rangle + \sum_{\gamma_2}\sum_{\gamma_1}\sum_k \langle\lambda_A\,|\,\gamma_2,k\rangle\langle\gamma_1,k\,|\,\lambda_B\rangle \times \langle\psi_{\gamma_2}\,|\,\nabla_{\mathbf{R}}\,|\,\psi_{\gamma_1}\rangle \tag{27}$$

which has the same form as $\hat{\mathbf{A}}^a$, see Eqs. (11)–(13). The coupled equations (6) and (25) are similar [they are equivalent via the unitary transformation (23)] except that (i) the GVV Hamiltonian $\hat{H}^{(\mathrm{GVV})}$ is nondiagonal and its diagonal elements are allowed to cross each other, whereas the $\epsilon_{\alpha m}^a(R)$'s are not; (ii) the field-dominated couplings $\hat{\mathbf{B}}_{\beta n,\alpha m}^a(\mathbf{R})$ in Eq. (12) in the dressed adiabatic picture show up mainly as the off-diagonal part of $\hat{H}^{(\mathrm{GVV})}$ in the GVV representation; and (iii) the quantity

$$\hat{\mathbf{B}}_{A,B}^{(\mathrm{GVV})}(\mathbf{R}) \equiv \frac{\mathbf{R}}{R}\sum_\gamma \sum_k \langle\lambda_A\,|\,\gamma k\rangle\frac{d}{dR}\langle\gamma k\,|\,\lambda_B\rangle$$

in Eq. (27) is small, unlike its counterpart $\hat{\mathbf{B}}_{\beta n,\alpha m}^a(\mathbf{R})$, even at pseudocrossings (to be seen later). The collision-dominated couplings

$$\hat{\mathbf{D}}_{A,B}^{(\mathrm{GVV})} \equiv \sum_{\gamma_2}\sum_{\gamma_1}\sum_k \langle\lambda_A\,|\,\gamma_2,k\rangle\langle\gamma_1,k\,|\,\lambda_B\rangle\langle\psi_{\gamma_2}\,|\,\nabla_{\mathbf{R}}\,|\,\psi_{\gamma_1}\rangle$$

of Eq. (27) in the GVV picture and $\hat{\mathbf{D}}_{\beta n,\alpha m}^a(\mathbf{R})$ of Eq. (13) in the adiabatic picture are connected simply by the unitary transformation defined by $\hat{\mathbf{U}}(R)$ of Eq. (22), or (23). When the collision-induced transition, e.g., the process (14), is negligibly small, we can safely drop the whole term with which the $\hat{\mathbf{A}}^{(\mathrm{GVV})}$ is associated in Eq. (24), and thus obtain the coupled equations,

$$i\frac{\partial}{\partial t}\chi_A^{(\mathrm{GVV})}(R(t)) = \sum_B \hat{H}_{A,B}^{(\mathrm{GVV})}(R)\chi_B^{(\mathrm{GVV})}(R) , \tag{28}$$

which have the same form as the exact diabatic coupled equations (15). Therefore, the GVV Hamiltonian $\hat{H}^{(\mathrm{GVV})}(R)$ plays the same role of the diabatic potential $\hat{V}(R)$ defined via Eqs. (17) and (18), or, in other words, the transformation matrix $\hat{U}(R)$ of Eq. (22) plays the same role of the unitary transformation $\hat{C}(R)$ defined by Eq. (18). We should remark here that although we have formally identified $\hat{U}(R)$ as $\hat{C}(R)$, in practice we never really need to evaluate the transformation matrix $\hat{U}(R)$ because the GVV Hamiltonian $\hat{H}^{(\mathrm{GVV})}$ can be constructed directly from the model-space wave functions $\{|\lambda_A\rangle\}$ in Eq. (20). Also, the DQMS eigenenergies $\{\epsilon_{\beta n}^a(R)\}$ can be obtained by simply diagonalizing the GVV Hamiltonian $\hat{H}^{(\mathrm{GVV})}(R)$. In the case that the collision-dominated couplings $\hat{\mathbf{D}}^a$, or $\hat{\mathbf{D}}^{(\mathrm{GVV})}$, are not small, we can always return to Eqs. (25) and solve the exact GVV coupled equations, although the latter are neither adiabatic nor diabatic in the sense defined via the matrix element of the operator $\nabla_{\mathbf{R}}$.[13]

The GVV coupled equations, i.e., (24) or (28), can be solved subject to the initial conditions

$$\chi_A^{(\mathrm{GVV})}(R(t)) \equiv \chi_{\alpha m}^{(\mathrm{GVV})}(R(t)) \to \delta_{\alpha\mu}\delta_{m0} \quad \text{as } t \to -\infty \tag{29}$$

with μ indexing the initial state of the colliding system before entering the laser field. The transition probability of finding the system initially in a field-free quasimolecular state $|\mu\rangle = \psi_\mu(\mathbf{r},\mathbf{R}(t=-\infty))$ and finally in a state $|\nu\rangle \equiv \psi_\nu(\mathbf{r},\mathbf{R}(t=+\infty))$ can be computed by the relation

$$P_{\mu\nu}(\rho,\mathbf{v}_0;\mathbf{E}_0,\omega) = \sum_{m=-\infty}^{\infty} |\chi_{\nu m}^{(\mathrm{GVV})}(R(t=+\infty))|^2 \tag{30}$$

for a set of specific parameters ρ, $\mathbf{v}_0$, $\mathbf{E}_0(\theta,\phi)$, and ω. To obtain the reaction cross section at fixed $\mathbf{v}_0$, $\mathbf{E}_0(\theta,\phi)$, and ω we integrate Eq. (30) over the impact parameters ρ and obtain

$$\sigma_{\mu\nu}(\mathbf{v}_0;\mathbf{E}_0,\omega) = 2\pi\int_0^\infty d\rho\,\rho P_{\mu\nu}(\rho,\mathbf{v}_0;\mathbf{E}_0,\omega) . \tag{31}$$

Finally, we need to average Eq. (31) over all possible orientations of the laser fields $\mathbf{E}(\theta,\phi)$ with respect to the collisional plane defined by $\mathbf{v}_0$ and the internuclear axis $\mathbf{R}$, namely,

$$\bar{\sigma}_{\mu\nu}(\mathbf{v}_0;|\mathbf{E}_0|,\omega)=\frac{1}{4\pi}\int d\Omega\,\sigma_{\mu\nu}(\mathbf{v}_0;\mathbf{E}_0(\theta,\phi),\omega)\ , \quad (32)$$

to compare with experimental measurements.

III. THE GVV TWO-STATE MODEL

In this section we consider only two quasimolecular states, say $|\alpha\rangle\equiv\psi_\alpha$ and $|\beta\rangle\equiv\psi_\beta$ with $E_\beta(R)>E_\alpha(R)$ at all R. The transition dipole moment between these two states is $\boldsymbol{\mu}_{\alpha\beta}\equiv\langle\alpha|\mathbf{r}|\beta\rangle$, while the effects of the permanent dipole moments will be ignored. The laser field is characterized by the amplitude $E_0(\theta,\phi)$ and the frequency ω which matches the energy defect $\Delta E(R)=E_\beta(R)-E_\alpha(R)$ at some finite internuclear separation R_x, i.e., $\omega=\Delta E(R_x)$. Assuming the system initially, before entering the laser field, is in the state $|\alpha\rangle$, the corresponding GVV Hamiltonian $\hat{H}^{(\mathrm{GVV})}_{2\times2}$ can be easily derived on a two-dimensional manifold M_2 spanned by two perturbed model-space wave functions $|\lambda_{\alpha0}\rangle$ and $|\lambda_{\beta,-1}\rangle$ of the forms

$$|\lambda_{\alpha0}\rangle=|\alpha,0\rangle+|\lambda^{(1)}_{\alpha0}\rangle+|\lambda^{(2)}_{\alpha0}\rangle+\cdots\ , \quad (33)$$

and

$$|\lambda_{\beta,-1}\rangle=|\beta,-1\rangle+|\lambda^{(1)}_{\beta,-1}\rangle+|\lambda^{(2)}_{\beta,-1}\rangle+\cdots\ , \quad (34)$$

where $|\lambda^{(n)}_{\alpha0}\rangle$ and $|\lambda^{(n)}_{\beta,-1}\rangle$ are the nth-order corrections of $|\lambda_{\alpha0}\rangle$ and $|\lambda_{\beta,-1}\rangle$, respectively. To the second order of the perturbed model-space wave functions, we can easily derive

$$|\lambda_{\alpha0}\rangle=\left[1-\frac{1}{2}\frac{b^2}{(\omega_0+\omega)^2}\right]|\alpha,0\rangle-\frac{b}{\omega_0+\omega}|\beta,1\rangle+\frac{b^2}{2\omega(\omega_0+\omega)}(|\alpha,2\rangle-|\alpha,-2\rangle)\ , \quad (35)$$

and

$$|\lambda_{\beta,-1}\rangle=\left[1-\frac{1}{2}\frac{b^2}{(\omega_0+\omega)^2}\right]|\beta,-1\rangle+\frac{b}{\omega_0+\omega}|\alpha,-2\rangle+\frac{b^2}{2\omega(\omega_0+\omega)}(|\beta,-3\rangle-|\beta,1\rangle)\ , \quad (36)$$

where

$$\omega_0=\omega_0(R)\equiv E_\beta(R)-E_\alpha(R)\ ,$$

and

$$b\equiv-\tfrac{1}{2}\boldsymbol{\mu}_{\alpha\beta}\cdot\mathbf{E}_0(\theta,\phi)$$

which is a function of $\mathbf{R}$, θ, and ϕ. Here we note that in obtaining Eqs. (35) and (36), the full normalization condition has been imposed on the model-space wave functions, i.e., $\langle\lambda_A|\lambda_B\rangle=\delta_{AB}+O(b^3)$. By using Eqs. (35) and (36), the GVV Hamiltonian $\hat{H}^{(\mathrm{GVV})}_{2\times2}$ can be evaluated to fifth order [it is a special feature of the GVV theory that when the model-space wave functions are accurate to nth order, the corresponding GVV Hamiltonian can be accurate to $(2n+1)$th order],[20,22] namely,

$$\hat{H}^{(\mathrm{GVV})}_{2\times2}(R)=\sum_{i=0}^{5}\hat{H}^{(i)}_{2\times2}(R)\ ,$$

where

$$[\hat{H}^{(0)}_{2\times2}]_{\alpha0,\alpha0}=E_\alpha(R)\ ,$$

$$[\hat{H}^{(0)}_{2\times2}]_{\beta-1,\beta-1}=E_\beta(R)-\omega\ ,$$

$$[\hat{H}^{(1)}_{2\times2}]_{\alpha0,\beta-1}=[\hat{H}^{(1)}_{2\times2}]^*_{\beta-1,\alpha0}=b\ ,$$

$$[\hat{H}^{(2)}_{2\times2}]_{\alpha0,\alpha0}=-[\hat{H}^{(2)}_{2\times2}]_{\beta-1,\beta-1}=-\frac{b^2}{\omega_0+\omega}\ , \quad (37)$$

$$[\hat{H}^{(3)}_{2\times2}]_{\alpha0,\beta-1}=[\hat{H}^{(3)}_{2\times2}]^*_{\beta-1,\alpha0}=-\frac{b^3}{(\omega_0+\omega)^2}\ ,$$

$$[\hat{H}^{(4)}_{2\times2}]_{\alpha0,\alpha0}=[\hat{H}^{(4)}_{2\times2}]_{\beta-1,\beta-1}=\frac{b^4}{(\omega_0+\omega)^3}\ ,$$

$$[\hat{H}^{(5)}_{2\times2}]_{\alpha0,\beta-1}=[\hat{H}^{(5)}_{2\times2}]^*_{\beta-1,\alpha0}=\frac{-\omega_0+\omega/2}{\omega^2(\omega_0+\omega)^2}b^5\ .$$

The nonvanishing matrix elements of the matrix $\hat{\mathbf{B}}^{(\mathrm{GVV})}$ of Eq. (27) can also be evaluated easily via the expression

$$\hat{\mathbf{B}}^{(\mathrm{GVV})}_{\alpha0,\beta-1}(R)=-\hat{\mathbf{B}}^{(\mathrm{GVV})*}_{\beta-1,\alpha0}(R)=\frac{b}{4\omega(\omega_0+\omega)^2}\frac{d}{dR}(b^2)\ . \quad (38)$$

It is seen from Eqs. (37) and (38) that if we neglect the collision-dominated coupling, i.e., $\hat{\mathbf{D}}^{(\mathrm{GVV})}$, in Eq. (24), the GVV coupling equations do not possess any nonsmooth components. Furthermore, the magnitude of the matrix elements of $\hat{\mathbf{A}}^{(\mathrm{GVV})}=\hat{\mathbf{B}}^{(\mathrm{GVV})}+\hat{\mathbf{D}}^{(\mathrm{GVV})}$ when compared with their counterparts in $\hat{\mathbf{H}}^{(\mathrm{GVV})}$ can be ignored. It is worth noting that the ordinary RWA approach amounts to considering only the first-order GVV Hamiltonian of Eq. (37), i.e., it neglects all anti-rotating effects; the quantity $\hat{\mathbf{B}}^{(\mathrm{GVV})}$ in the RWA limit vanishes exactly.

For illustration, we consider the two states $|3d\sigma\rangle$ and $|4f\sigma\rangle$ for the process (14) illuminated by a strong laser field of intensity $I=10$ TW/cm^2, and of wavelength $\lambda=2000$ Å. We further assume that the laser field $\mathbf{E}_0$ is in the $\hat{\mathbf{z}}$ direction, i.e., $\mathbf{E}_0\|\hat{\mathbf{z}}\|\mathbf{v}_0$ and $|\mathbf{v}_0|=1.0\times10^7$ cm/s. The frequency ω of the laser field will match the energy defect $\Delta E(R_x)=E_{4f\sigma}(R_x)-E_{3d\sigma}(R_x)$ at $R_x\approx7$ a.u. At the impact parameter $\rho=1$ a.u., we present in Fig. 4 the two diagonal elements of the GVV Hamiltonian $\hat{H}^{(\mathrm{GVV})}_{2\times2}(R)$, as a function of R, which cross over each other around $R_x\approx7$ a.u. For a closer examination, in Fig. 5, we plot both RWA and GVV diagonal parts and find that the location of the intersection of the two RWA potentials $E_{4f\sigma}(R)-\omega$ and $E_{3d\sigma}(R)$ does not coincide with that of the two GVV potentials $[\hat{H}^{(\mathrm{GVV})}_{2\times2}]_{\alpha0,\alpha0}$ and $[\hat{H}^{(\mathrm{GVV})}_{2\times2}]_{\beta-1,\beta-1}$ with $\alpha=3d\sigma$ and $\beta=4f\sigma$. The shift of the cross point from RWA's to GVV's is the well-known Bloch-Siegert shift[23] which plays an important role in the resonant single-photon process of a two-state system in the presence of a strong laser field. In Fig. 6 we present the off-diagonal part $[\hat{H}^{(\mathrm{GVV})}_{2\times2}]_{\alpha0,\beta-1}$ along with the quantity $|\dot{\mathbf{R}}\cdot\hat{\mathbf{B}}^{(\mathrm{GVV})}_{\alpha0,\beta-1}|$. It is found that the latter is several or-

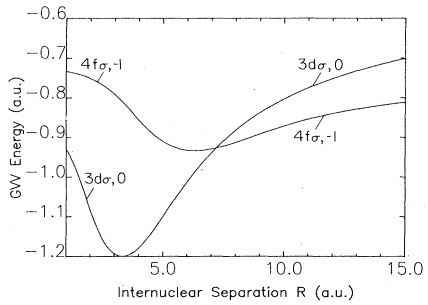

FIG. 4. The GVV potential energies of the two-state GVV model. The two GVV model-space wave functions considered here are $|\lambda_1\rangle \equiv |\lambda_{3d\sigma,0}\rangle$ and $|\lambda_2\rangle \equiv |\lambda_{4f\sigma,-1}\rangle$. Data are calculated at the same conditions as those described in Fig. 3.

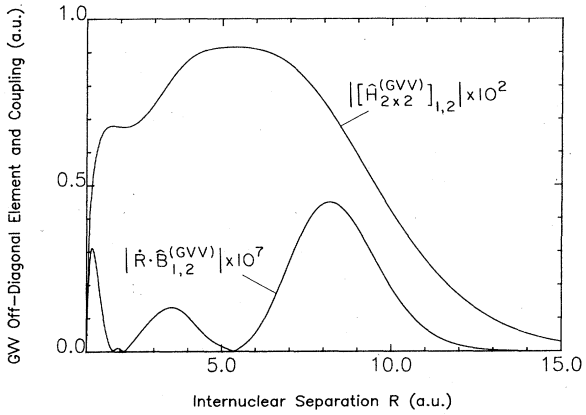

FIG. 6. GVV off-diagonal element $[\hat{H}^{(GVV)}_{2\times2}]_{1,2}$ and the corresponding $|\dot{\mathbf{R}}\cdot\hat{\mathbf{B}}^{(GVV)}_{1,2}|$, see Eq. (38), of the two-state GVV model. For further explanation see the caption of Fig. 4.

ders of magnitude smaller than the former and thus can be safely dropped. When the collision-induced coupling is not important, such as in process (14), we are therefore justified in using the GVV coupled equations (28) to study the dynamics of slow atomic collisions in the presence of a strong field. The results presented in Sec. IV are based exclusively on Eq. (28).

IV. RESULTS AND DISCUSSIONS

In this section we shall evaluate the charge-transfer transition probabilities and total cross sections for the laser-assisted process (14). For simplicity, we shall assume that (i) the impact velocity $|\mathbf{v}_0|$ is small enough that the collision-induced coupling can be neglected, (ii) the laser field is oscillating in the $\hat{\mathbf{z}}$ direction which is chosen as parallel to the impact velocity $\mathbf{v}_0$, and (iii) all of permanent dipole moments of the quasimolecular states are negligible. We have seen (Fig. 2) that the correlation diagram of the DQMS potential energies of the $(LiH)^{3+}$ system in the presence of a strong laser field is extremely complicated. In the course of the collision, the number of dressed-quasimolecular states coupled strongly to the entrance channel, here the unperturbed DQM state $|3d\sigma,0\rangle$, is large. Strong couplings can be traced by avoided crossings which indicate possible transitions between states caused by single- or multiple-photon resonances. For the range of laser frequencies to be studied below, from 1500 to 3000 Å, the field-induced transitions due to one-photon resonant process dominate over various types of multiple-photon processes. When assuming that single-photon resonant transitions prevail in the collision, we can easily identify the DQMS closely coupled to the entrance channel, and construct the GVV Hamiltonian $\hat{H}^{(GVV)}$ accordingly.

In the following we consider three different GVV model spaces, namely, (i) M_2, the 2-state model, spanned by $|\lambda_{3d\sigma,0}\rangle$, and $|\lambda_{4f\sigma,-1}\rangle$; (ii) M_5, the 5-state model, spanned by $|\lambda_{3d\sigma,0}\rangle$, $|\lambda_{4f\sigma,-1}\rangle$, $|\lambda_{3d\pi,-1}\rangle$, $|\lambda_{3p\sigma,-1}\rangle$, and $|\lambda_{3p\pi,-1}\rangle$; and, finally, (iii) M_{15}, the 15-state model, spanned by $|\lambda_{3d\sigma,1}\rangle$, $|\lambda_{4f\sigma,0}\rangle$, $|\lambda_{3d\pi,0}\rangle$, $|\lambda_{3p\sigma,0}\rangle$, $|\lambda_{3p\pi,0}\rangle$, $|\lambda_{3d\sigma,0}\rangle$, $|\lambda_{4f\sigma,-1}\rangle$, $|\lambda_{3d\pi,-1}\rangle$, $|\lambda_{3p\sigma,-1}\rangle$, $|\lambda_{3p\pi,-1}\rangle$, $|\lambda_{3d\sigma,-1}\rangle$, $|\lambda_{4f\sigma,-2}\rangle$, $|\lambda_{3d\pi,-2}\rangle$, $|\lambda_{3p\sigma,-2}\rangle$, and $|\lambda_{3p\pi,-2}\rangle$ (see Fig. 2), assuming the initial state is $|3d\sigma,0\rangle$ which asymptotically assigns the electron to the ground state of the hydrogen atom. The four quasimolecular states $4f\sigma$, $3d\pi$, $3p\sigma$, and $3p\pi$ all asymptotically associate with the state $Li^{2+}(n=3)$, the charge-transfer channel. The two-state model consisting of the quasimolecular states $3d\sigma$, as the entrance channel, and $4f\sigma$, as the final channel, has been studied in the RWA limit, and, along with perturbation theory, yields linear dependence of the charge capture cross section on both the laser intensity and the reciprocal of the impact velocity $1/v_0$.[11(b)] Although it is true under certain circumstances that the two states discussed above prevail in process (14), we find, as is shown below, that the five-state model will be much more satisfactory when all dynamical factors are taken into consideration. This five-state model allows the charge transfer to take place at some moderate internuclear separations, see Figs. 3(a) and 3(b), depending on the laser frequency. The more complete 15-state model accounts for all one-photon resonant processes, absorption or emission, encountered during the collision, see Fig. 2, The two-state GVV Hamiltonian $\hat{H}^{(GVV)}_{2\times2}$ has been illustrated in Sec. III, while the 5- and 15-state GVV Hamiltonians $\hat{H}^{(GVV)}_{5\times5}$ and $\hat{H}^{(GVV)}_{15\times15}$, respectively, are presented in Appendixes A and B.

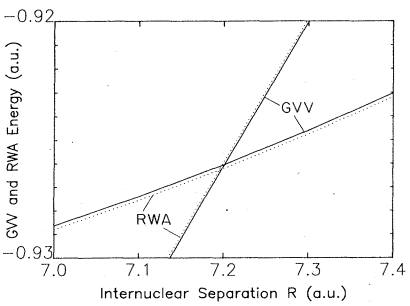

FIG. 5. Comparison between the two-state GVV (solid) and RWA (dotted) potential energies at the conditions of Fig. 4.

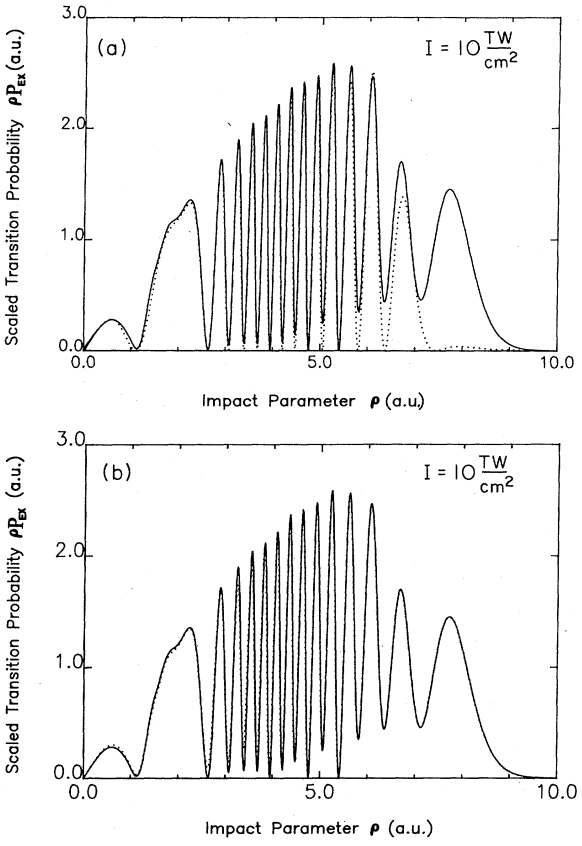

FIG. 7. Scaled charge-transfer transition probabilities, as functions of the impact parameter ρ, of the GVV 2-state (2S) [dotted curve in (a)], GVV 5-state (5S) [solid curve in (a) and (b)], and GVV 15-state (15S) [dotted curve in (b)] calculations at impact velocity $|\mathbf{v}_0| = 1.0\times10^7$ cm/s, intensity $I=10$ TW/cm^2, and wavelength $\lambda=2000$ Å for the process shown in Eq. (14).

In Fig. 7 we show the scaled transition probabilities, ρP_{ex}, of the charge-exchange process (14) as functions of the impact parameter ρ, at laser intensity $I=10$ TW/cm^2, wavelength $\lambda=2000$ Å, and impact velocity $|\mathbf{v}_0| = 1.0\times10^7$ cm/s. Results of numerical integrations of Eq. (28) for the 2S and 5S models are presented in Fig. 7(a) which shows that the two results agree quite well at impact parameters ρ less than about 7 a.u., whereas they differ significantly at larger impact parameters. Figure 3(a) shows two groups of avoided crossings of the one-photon resonant nature (the rest involves two photons, one absorption plus one emission): (i) four far-side crossings between the DQM state $|\lambda_{3d\sigma,0}\rangle$ and states $|\lambda_{4f\sigma,-1}\rangle$, $|\lambda_{3d\pi,-1}\rangle$, $|\lambda_{3p\sigma,-1}\rangle$, and $|\lambda_{3p\pi,-1}\rangle$, respectively, ranging from about 6 to 10 a.u., and (ii) three inner crossings between the DQM state $|\lambda_{3d\sigma,0}\rangle$ and states $|\lambda_{3p\pi,-1}\rangle$, $|\lambda_{3p\sigma,-1}\rangle$, and $|\lambda_{3d\pi,-1}\rangle$, respectively, ranging from about 1.5 to 2.5 a.u. Figure 3(b) shows the degree of the coupling between each pair of states: the lower and more stretched the profile of the nonadiabatic coupling is, the stronger the coupling is [this is shown in Fig. 3(a) as greater splitting of wider area between the avoided crossed curves]. From Eq. (31) it is understood that as far as the total cross section is concerned the coupling at larger internuclear separation contributes relatively more than that at smaller separation because of the weighting factor ρ—the impact parameter. Thus the allowance for more reaction channels in the 5S model than in the 2S model results in the large difference between the two calculations, particularly at larger impact parameters. Some differences between the 2S and 5S models are also seen at small impact parameters, but these have been downplayed by the scaling factor ρ. Here we should remark that the couplings between $3d\sigma$ and states other than $4f\sigma$ at larger separations (≥ 6 a.u.) can be gradually turned off, before that between the $3d\sigma$ and $4f\sigma$ states, by increasing the wavelength of the laser field, cf. Fig. 1(b). The 2S model will then become a sufficiently good approximation. In the 15S model, see Fig. 7(b), we found that the inclusion of more channels—which come in mainly at small internuclear separations—than in the 5S one (see Fig. 2) does not significantly change the charge-exchange transition probability at any range of the impact parameters, at the intensity and the wavelength under study. If we further increase the intensity of the laser field to 100 TW/cm^2, we then observe some difference, at small impact parameters, between results of the 5S and 15S models; see Fig. 8. Nevertheless the total cross sections obtained from the 5S model remain quite satisfactory when compared with the 15S model even at this high field intensity.

In Figs. 9 and 10, the total cross sections, Eq. (31), are presented as functions of the laser intensity I at impact velocity $|\mathbf{v}_0| = 1.0\times10^7$ cm/s and at wavelengths of 2000 and 2700 Å, respectively. Along with results of the GVV 2S, 5S, and 15S models, also shown are results based on first-order perturbation theory within the 2S model, here called 2SP1. In general, we see that the 5S and 15S results agree well even at rather high intensity, while the 2S results show good agreement with the 5S and 15S at larger wavelengths (see also Fig. 11). At shorter wavelengths, e.g., $\lambda=2000$ Å, the 2S results are inaccurate even at rather low intensities, e.g., 1 TW/cm^2. The 2SP1

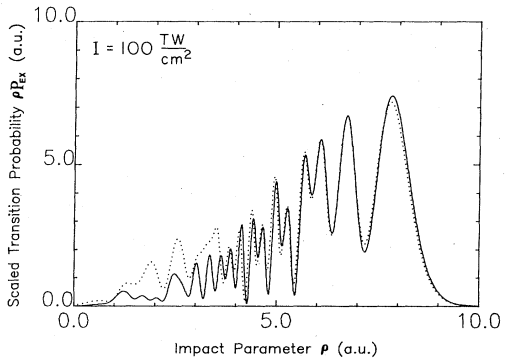

FIG. 8. Scaled charge-transfer transition probabilities, as functions of the impact parameter ρ, of the GVV 5S (solid curve) and GVV 15S (dotted curve) calculations at impact velocity $|\mathbf{v}_0| = 1.0\times10^7$ cm/s, intensity $I=100$ TW/cm^2, and wavelength $\lambda=2000$ Å for the process shown in Eq. (14).

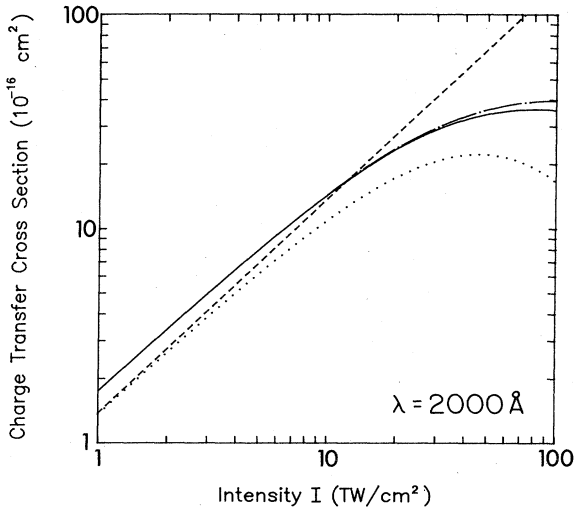

FIG. 9. The total charge-transfer cross sections, as functions of the laser field intensity I, of the GVV 5S (solid), GVV 15S (dashed-dotted), and GVV 2S (dotted) calculations at impact velocity $|\mathbf{v}_0| = 1.0\times10^7$ cm/s and wavelength $\lambda = 2000$ Å for the process shown in Eq. (14). Dashed curve (2SP1) is based on the first-order perturbation calculation within the GVV 2S model.

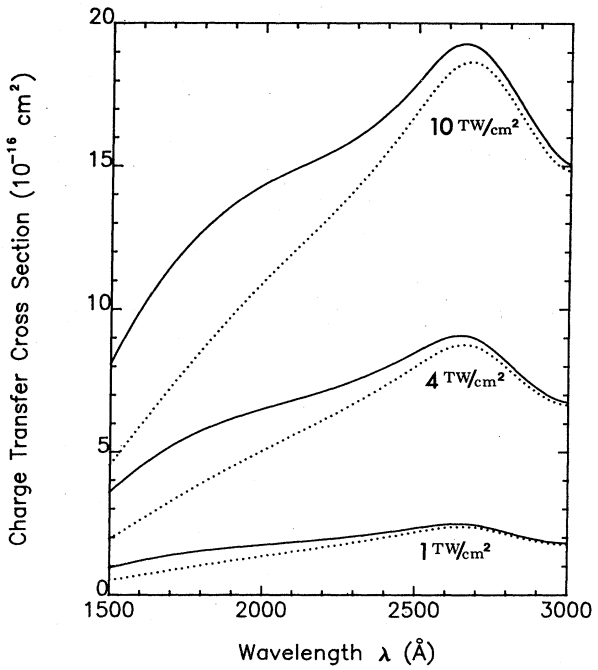

FIG. 11. The total charge-transfer cross sections, as functions of the wavelength λ, of the GVV 5S (solid) and 2S (dotted) calculations at the impact velocity $|\mathbf{v}_0| = 1.0\times10^7$ cm/s and laser intensities $I = 1.0$, 4.0, and 10.0 TW/cm^2 for the process shown in Eq. (14).

calculations, which show the linear dependence of the total cross section on the laser intensity, underestimate the cross section at the lower intensity and overestimate it at the higher one (which is obvious) except when the intensity is very low and the wavelength is relatively large, see Fig. 10.

The behavior of the charge-exchange cross sections as we vary the laser wavelength λ is shown for the 2S and 5S models in Fig. 11 at impact velocity $|\mathbf{v}_0| = 1.0\times10^7$ cm/s and at three different intensities: 1.0, 4.0, and 10.0 TW/cm^2. It is rather interesting to see that at lower intensity the curve is broad (flatter), whereas at higher intensity the curve shows a pronounced peak around $\lambda = 2700$ Å. In general the differences between the 2S and 5S results are greater at higher intensities and at smaller wavelengths as discussed above.

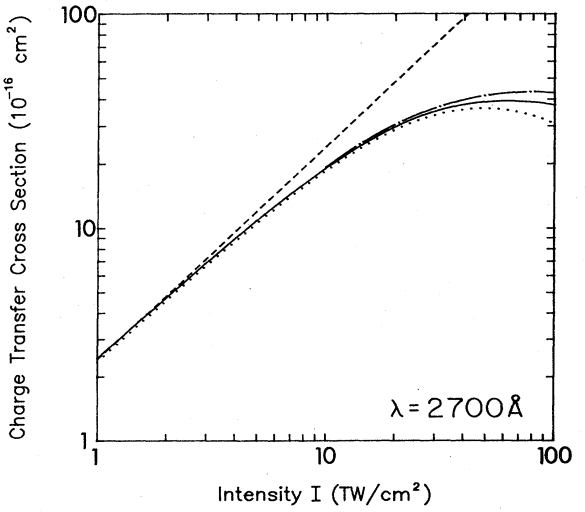

FIG. 10. Same as Fig. 9, but at the wavelength $\lambda = 2700$ Å.

From the results presented so far we see that for the laser-assisted charge-transfer process (14), the GVV five-state model provides a good approximation for a wide range of laser intensities and wavelengths at small impact velocities. In other words, the couplings within the electric dipole approximation between the quasimolecular $3d\sigma$ state and the $4f\sigma$, $3d\pi$, $3p\sigma$, and $3p\pi$ states at some larger internuclear separations where the transition dipole moments are still important, are the main driving mechanism causing charge transfer in the process.

V. CONCLUSIONS

We have presented a nonperturbative semiclassical DQMS approach for the general treatment of multichannel slow ion-atom collisions in the presence of intense laser fields. The implementation of the GVV perturbation theory in the Floquet Hamiltonian allows the reduction of the number of effective coupled channels, and in addition, provides a numerically stable algorithm for minimizing the large field-induced radical couplings. This yields a set of GVV coupled equations which offers some computational advantages over either the adiabatic or the diabatic DQMS approaches previously proposed.[13] The coupled GVV-DQMS approach is extended to a detailed study of the laser-assisted charge-exchange process of the bare

lithiums slowly impinging on ground-state neutral hydrogen atoms. It is found that a five-GVV-DQMS basis is adequate for the description of the processes for a wide range of laser intensities and wavelengths. Extension of the approach to the study of several laser-assisted charge-transfer processes involving multiphoton absorptions is in progress.

ACKNOWLEDGMENTS

This work was supported in part by the U.S. Department of Energy (Division of Chemical Sciences), by the University of Kansas General Research Fund, and by the Alfred P. Sloan Foundation (for S.-I C.). Acknowledgment is also made to the Donors of the Petroleum Research Fund, administered by the American Chemical Society, for partial support of this work. One of the authors (S.-I C.) would like to acknowledge financial support from the JILA Visiting Fellow Program.

APPENDIX A: THE FIVE-STATE GVV HAMILTONIAN $\hat{H}^{(\mathrm{GVV})}_{5\times5}(R)$

Considering the manifold M_5 spanned by the model-space wave functions $|\lambda_{1,0}\rangle \equiv |\lambda_{3d\sigma,0}\rangle$, $|\lambda_{2,-1}\rangle \equiv |\lambda_{4f\sigma,-1}\rangle$, $|\lambda_{3,-1}\rangle \equiv |\lambda_{3d\pi,-1}\rangle$, $|\lambda_{4,-1}\rangle \equiv |\lambda_{3p\sigma,-1}\rangle$, and $|\lambda_{5,-1}\rangle \equiv |\lambda_{3p\pi,-1}\rangle$ of the system $(\mathrm{LiH})^{3+}$ in the presence of a strong laser field, we can construct the corresponding GVV Hermitian Hamiltonian $\hat{H}^{(\mathrm{GVV})}_{5\times5}(R)$ to the third order as follows:

$$\hat{H}^{(\mathrm{GVV})}_{5\times5}=\hat{H}^{(0)}_{5\times5}+\hat{H}^{(1)}_{5\times5}+\hat{H}^{(2)}_{5\times5}+\hat{H}^{(3)}_{5\times5}\ , \tag{A1}$$

where the nonzero components of different orders of corrections are

$$\begin{aligned}&[\hat{H}^{(0)}_{5\times5}]_{10,10}=E_1\equiv E_{3d\sigma}\ ,\\ &[\hat{H}^{(0)}_{5\times5}]_{\alpha,-1}=E_\alpha-\omega\quad(\alpha=2,3,4,5)\ ,\end{aligned} \tag{A2}$$

with

$$E_2\equiv E_{4f\sigma},\ E_3\equiv E_{3d\pi},\ E_4\equiv E_{3p\sigma},\ E_5\equiv E_{3p\pi}\ ;$$

$$[\hat{H}^{(1)}_{5\times5}]_{10,\alpha-1}=b_{1\alpha}\quad(\alpha=2,3,4,5,)\ ; \tag{A3}$$

$$[\hat{H}^{(2)}_{5\times5}]_{10,10}=\sum_{\alpha=2}^{5}\frac{|b_{1\alpha}|^2}{E_1-E_\alpha-\omega}\ ,$$

$$[\hat{H}^{(2)}_{5\times5}]_{\alpha-1,\beta-1}=\tfrac{1}{2}b_{1\alpha}b^*_{1\beta}\left[\frac{1}{E_\alpha-E_1+\omega}+\frac{1}{E_\beta-E_1+\omega}\right]\qquad(\alpha,\beta\neq1)\ ; \tag{A4}$$

and

$$[\hat{H}^{(3)}_{5\times5}]_{10,\alpha-1}=-\tfrac{1}{2}b_{1\alpha}\sum_{\beta=2}^{5}|b_{1\beta}|^2\left[\frac{1}{(E_1-E_\beta-\omega)^2}+\frac{1}{(E_\beta-E_1+\omega)(E_\alpha-E_1+\omega)}\right]\quad(\alpha=2,3,4,5)\ . \tag{A5}$$

Here the transition dipole moment $b_{1\alpha}(R)$ is defined as

$$b_{1\alpha}(R)=b^*_{\alpha1}(R)=-\tfrac{1}{2}\langle 1|\mathbf{r}|\alpha\rangle\cdot\mathbf{E}_0(\theta,\phi)\ , \tag{A6}$$

where $\mathbf{r}$ is the position of the electron and $\mathbf{E}_0(\theta,\phi)$ is the amplitude of the laser field whose orientation is described by the polar and azimuthal angles θ and ϕ, respectively, with respect to the impact velocity $\mathbf{v}_0$. The permanent dipole moments of all quasimolecular states are neglected.

APPENDIX B: THE 15-STATE GVV HAMILTONIAN $\hat{H}^{(\mathrm{GVV})}_{15\times15}$

Considering the manifold M_{15} spanned by the model-space wave functions $|\lambda_{3d\sigma,1}\rangle$, $|\lambda_{4f\sigma,0}\rangle$, $|\lambda_{3d\pi,0}\rangle$, $|\lambda_{3p\sigma,0}\rangle$, $|\lambda_{3p\pi,0}\rangle$, $|\lambda_{3d\sigma,0}\rangle$, $|\lambda_{4f\sigma,-1}\rangle$, $|\lambda_{3d\pi,-1}\rangle$, $|\lambda_{3p\sigma,-1}\rangle$, $|\lambda_{3p\pi,-1}\rangle$, $|\lambda_{3d\sigma,-1}\rangle$, $|\lambda_{4f\sigma,-2}\rangle$, $|\lambda_{3d\pi,-2}\rangle$, $|\lambda_{3p\sigma,-2}\rangle$, and $|\lambda_{3p\pi,-2}\rangle$ for the $(\mathrm{LiH})^{3+}$ system in the presence of a strong laser field, the corresponding GVV Hamiltonian, to the first order of perturbation theory, adopted in the calculation can be written as

$$\hat{H}^{(\mathrm{GVV})}_{15\times15}=\begin{bmatrix}
3d\sigma,1 & b_{12} & b_{13} & b_{14} & b_{15} & 0 & 0 & 0 & 0 & 0 & 0 & 0 & 0 & 0 & 0\\
 & 4f\sigma,0 & 0 & 0 & 0 & 0 & 0 & b_{23} & b_{24} & b_{25} & b_{21} & 0 & 0 & 0 & 0\\
 & & 3d\pi,0 & 0 & 0 & 0 & b_{32} & 0 & b_{34} & b_{35} & b_{31} & 0 & 0 & 0 & 0\\
 & & & 3p\sigma,0 & 0 & 0 & b_{42} & b_{43} & 0 & b_{45} & b_{41} & 0 & 0 & 0 & 0\\
 & & & & 3p\pi,0 & 0 & b_{52} & b_{53} & b_{54} & 0 & b_{51} & 0 & 0 & 0 & 0\\
 & & & & & 3d\sigma,0 & b_{12} & b_{13} & b_{14} & b_{15} & 0 & 0 & 0 & 0 & 0\\
 & & & & & & 4f\sigma,-1 & 0 & 0 & 0 & 0 & 0 & b_{23} & b_{24} & b_{25}\\
 & & & & & & & 3d\pi,-1 & 0 & 0 & 0 & b_{32} & 0 & b_{34} & b_{35}\\
 & & & & & & & & 3p\sigma,-1 & 0 & 0 & b_{42} & b_{43} & 0 & b_{45}\\
 & & & & & & & & & 3p\pi,-1 & 0 & b_{52} & b_{53} & b_{54} & 0\\
 & & & & & & & & & & 3d\sigma,-1 & b_{12} & b_{13} & b_{14} & b_{15}\\
 & & & & & & & & & & & 4f\sigma,-2 & 0 & 0 & 0\\
 & & & & & & & & & & & & 3d\pi,-2 & 0 & 0\\
 & & & & & & & & & & & & & 3p\sigma,-2 & 0\\
 & & & & & & & & & & & & & & 3p\pi,-2
\end{bmatrix}, \tag{B1}$$

which is a Hermitian matrix. Here the quantity $b_{\alpha\beta}$ is defined as

$$b_{\alpha\beta}=-\tfrac{1}{2}\langle\alpha\,|\,\mathbf{r}\,|\,\beta\rangle\cdot\mathbf{E}_0(\theta,\phi)\ ,$$

where indices α and β range from 1 to 5, denoting, respectively, the quasimolecular states $3d\sigma$, $4f\sigma$, $3d\pi$, $3p\sigma$, and $3p\pi$ of the $(LiH)^{3+}$ system. We note that in constructing $\hat{H}^{(GVV)}_{15\times15}$ of Eq. (B1), (i) we have neglected all permanent dipole moments of quasimolecular states, and (ii) we have used the truncated total Floquet Hamiltonian $\hat{H}_F$ as the GVV Hamiltonian for the reason that the basis which spans the manifold M_{15} is sufficiently large so that higher-order corrections to $\hat{H}^{(GVV)}_{15\times15}$ will not be appreciable under the physical conditions considered in this paper.

---

*Permanent address: Department of Mathematics, University of Nottingham, Nottingham, NG7 2RD, England.
†Permanent address.

[1]See, for example, R. C. Isler and E. C. Crume, Phys. Rev. Lett. **41**, 1296 (1978).
[2](a) R. H. Dixon, J. F. Seely, and R. C. Elton, Phys. Rev. Lett. **40**, 122 (1978); (b) A. V. Vinogrudov and I. I. Sobelman, Zh. Eksp. Teor. Fiz. **63**, 2113 (1972) [Sov. Phys.—JETP **36**, 1115 (1973)]; (c) W. H. Louisell, M. O. Scully, and W. B. McKnight, Phys. Rev. A **11**, 989 (1975).
[3]S. I. Yakovlenko, Kvant. Elektron (Moscow) **5**, 259 (1978) [Sov. J. Quantum Electron. **8**, 151 (1978)].
[4]W. R. Green, M. D. Wright, J. F. Young, and S. E. Harris, Phys. Rev. Lett. **43**, 120 (1979).
[5]J. F. Seely and R. C. Elton, U.S. Naval Research Laboratory Memorandum Report No. 4317, 1980 (unpublished).
[6]R. Z. Vitlina, A. V. Chaplik, and M. V. Entin, Zh. Eksp. Teor. Fiz. **67**, 1667 (1974) [Sov. Phys.—JETP **40**, 829 (1975)].
[7]D. A. Copeland and C. L. Tang, J. Chem. Phys. **65**, 3161 (1976); **66**, 5126 (1977).
[8]L. I. Gudzenko and S. V. Yakovlenko, Zh. Tekh. Fiz. **45**, 234 (1975) [Sov. Phys.—Tech. Phys. **20**, 150 (1975)].
[9]E. A. Andreev and A. S. Prostner, Zh. Eksp. Teor. Fiz. **76**, 1969 (1979) [Sov. Phys.—JETP **49**, 998 (1979)].
[10]J. F. Seely, J. Chem. Phys. **75**, 3321 (1981).
[11](a) L. F. Errea, L. Méndez, and A. Riera, J. Chem. Phys. **79**, 4221 (1983); (b) Chem. Phys. Lett. **104**, 401 (1984).
[12]Y. P. Hsu, M. Kimura, and R. E. Olson, Phys. Rev. A **31**, 576 (1985).
[13]T. S. Ho, S.-I Chu, and C. Laughlin, J. Chem. Phys. **81**, 788 (1984).
[14]S.-I Chu, Chem. Phys. Lett. **70**, 205 (1980).
[15](a) T. F. George, J. Phys. Chem. **86**, 10 (1982), and references therein; (b) N. M. Kroll and K. M. Watson, Phys. Rev. A **13**, 1018 (1976); (c) A. M. Lau, *ibid.* **13**, 139 (1976).
[16](a) J. H. Shirely, Phys. Rev. B **138**, 979 (1965); (b) D. R. Dion and J. O. Hirschfelder, Adv. Chem. Phys. **35**, 265 (1976).
[17]For a recent review, see, S.-I Chu, Adv. At. Mol. Phys. (to be published).
[18](a) F. T. Smith, Phys. Rev. **179**, 111 (1969); (b) T. G. Heil and A. Dalgarno, J. Phys. B **12**, L557 (1979).
[19](a) B. Kirtman, J. Chem. Phys. **49**, 3890 (1968); (b) **75**, 798 (1981).
[20](a) P. R. Certain and J. O. Hirschfelder, J. Chem. Phys. **52**, 5977 (1970); (b) J. O. Hirschfelder, Chem. Phys. Lett. **54**, 1 (1978); P. K. Aravind and J. O. Hirschfelder, J. Phys. Chem. **88**, 4788 (1984).
[21]The field-free quasimolecular electronic energies and their transition dipole moments for the $(LiH)^{3+}$ system are calculated using the conventional method described for example in the following reference: T. Winter and N. F. Lane, Phys. Rev. A **17**, 66 (1978), and references therein.
[22]T. S. Ho and S.-I Chu, Phys. Rev. A **31**, 659 (1985).
[23]See, for example, L. Allen and J. H. Eberly, *Optical Resonance and the Two-Level Atoms* (Wiley, New York, 1975), Chap. 2.